

RESEARCH ARTICLE

IGFBP2 enhances adipogenic differentiation potentials of mesenchymal stem cells from Wharton's jelly of the umbilical cord *via* JNK and Akt signaling pathways

Yuejun Wang¹, Yunsong Liu¹, Zhipeng Fan², Dayong Liu², Fu Wang^{3*}, Yongsheng Zhou^{1,4*}

1 Department of Prosthodontics, Peking University School and Hospital of Stomatology, Beijing, China, **2** Laboratory of Molecular Signaling and Stem Cells Therapy, Beijing Key Laboratory of Tooth Regeneration and Function Reconstruction, Capital Medical University School of Stomatology, Beijing, China, **3** Department of Oral Basic Science, School of Stomatology, Dalian Medical University, Liaoning, China, **4** National Engineering Laboratory for Digital and Material Technology of Stomatology, Beijing, China

* kqzhouysh@hsc.pku.edu.cn (ZY); dywangfu@gmail.com (WF)



OPEN ACCESS

Citation: Wang Y, Liu Y, Fan Z, Liu D, Wang F, Zhou Y (2017) IGFBP2 enhances adipogenic differentiation potentials of mesenchymal stem cells from Wharton's jelly of the umbilical cord *via* JNK and Akt signaling pathways. PLoS ONE 12(8): e0184182. <https://doi.org/10.1371/journal.pone.0184182>

Editor: Joshua M. Hare, University of Miami School of Medicine, UNITED STATES

Received: January 3, 2017

Accepted: August 18, 2017

Published: August 31, 2017

Copyright: © 2017 Wang et al. This is an open access article distributed under the terms of the [Creative Commons Attribution License](https://creativecommons.org/licenses/by/4.0/), which permits unrestricted use, distribution, and reproduction in any medium, provided the original author and source are credited.

Data Availability Statement: All relevant data are within the paper and its Supporting Information files.

Funding: This work was supported by grants from the National Natural Science Foundation of China (No. 81170937), the Project for Culturing Leading Talents in Scientific and Technological Innovation of Beijing (Z171100001117169), and the Liaoning Natural Science Foundation (2013023014 to FW).

Abstract

Mesenchymal stem cell (MSC)-mediated tissue engineering represents a promising strategy to address adipose tissue defects. MSCs derived from Wharton's jelly of the umbilical cord (WJCMSCs) may serve as an ideal source for adipose tissue engineering due to their abundance, safety profile, and accessibility. How to activate the directed differentiation potentials of WJCMSCs is the core point for their clinical applications. A thorough investigation of mechanisms involved in WJCMSC adipogenic differentiation is necessary to support their application in adipose tissue engineering and address shortcomings. Previous study showed, compared with periodontal ligament stem cells (PDLSCs), WJCMSCs had a weakened adipogenic differentiation potentials and lower expression of insulin-like growth factor binding protein 2 (*IGFBP2*). *IGFBP2* may be involved in the adipogenesis of MSCs. Generally, *IGFBP2* is involved in regulating biological activity of insulin-like growth factors, however, its functions in human MSCs are unclear. Here, we found *IGFBP2* expression was upregulated upon adipogenic induction, and that *IGFBP2* enhanced adipogenic differentiation of WJCMSCs and BMSCs. Moreover, *IGFBP2* increased phosphorylation of c-Jun N-terminal kinase (p-JNK) and p-Akt, and activated JNK or Akt signaling significantly promoted adipogenic differentiation of MSCs. Furthermore, inhibitor-mediated blockage of either JNK or Akt signaling dramatically reduced *IGFBP2*-mediated adipogenic differentiation. And the JNK inhibitor, SP600125 markedly blocked *IGFBP2*-mediated Akt activation. Moreover, *IGFBP2* was negatively regulated by *BCOR*, which inhibited adipogenic differentiation of WJCMSCs. Overall, our results reveal a new function of *IGFBP2*, providing a novel insight into the mechanism of adipogenic differentiation and identifying a potential target mediator for improving adipose tissue engineering based on WJCMSCs.

Competing interests: The authors have declared that no competing interests exist.

Abbreviations: Akt, protein kinase B; AM, adipose-inducing medium; AP2 α , activating enhancer binding protein 2 alpha; ASCs, adipose-derived stem cells; BCOR, BCL6 corepressor; BMSCs, bone marrow mesenchymal stem cells; CD36, 36; CEBPA, CCAAT/enhancer-binding protein α ; CREB, cAMP response element-binding protein; ERK, extracellular regulated protein kinases; GAPDH, glyceraldehyde-3-phosphate dehydrogenase; IGF, insulin-like growth factor; IGFBP, insulin-like growth factor binding protein; JNK, c-Jun N-terminal kinase; LPL, lipoprotein lipase; MAPK, mitogen-activated protein kinase; MSCs, mesenchymal stem cells; OFCD, oculo-facio-cardio-dental; PDLSCs, periodontal ligament stem cells; PM, proliferation medium; PPAR γ , peroxisome proliferator-activated receptor γ ; SCAPs, stem cells from apical papilla; WJCMSCs, Wharton's jelly of the umbilical cord mesenchymal stem cells.

Introduction

Adipose tissue plays an essential role in the maintenance of organ contours, energy storage, metabolic balance, and immune regulation through exocrine hormones and fat cell factors. Adipose tissue defects due to tumor resection, trauma, or hereditary and congenital diseases usually lead to loss of fat tissue, poor appearance and local disordered regulatory function. A major clinical challenge is that traditional treatments such as prosthetic appliance, plastic and reconstructive surgery and fat grafting do not effectively restore adipose tissue. Adipose tissue engineering and cell-based therapies represent novel and promising approaches for regenerating adipose tissue.

MSCs have been isolated from various tissues, including bone marrow, adipose tissue, vascular tissue, dental tissue, craniofacial tissue, and umbilical cord [1–7]. With their convenient isolation, low immunogenicity, and ability to transdifferentiate, MSCs are considered a promising therapeutic approach for tissue regeneration [1,4,5,8,9]. WJCMSCs, which are isolated from neonatal umbilical cord tissue, are a plentiful, cost-effective, and biologically safe source of stem cells and show the significant potential for regenerative medicine [9–12]. As studied dental-derived stem cell population, PDLSCs which own the higher stemness features and preferable multi-differentiation properties, are the ideal seeding cells for tissue regeneration [8,13,14]. However, some researches suggested that compared with PDLSCs, unmodified WJCMSCs with their weaker stemness features might not be ideal seed cells for tissue regeneration [8,15]. A crucial issue for WJCMSCs-mediated adipose tissue regeneration is how to activate adipogenic differentiation and enhance regenerative ability.

As the essential member of insulin-like growth factor (IGF) axis, insulin-like growth factor binding proteins (IGFBPs) are homologs with high structural similarity but distinct functionalities. They all have similar N-terminal and C-terminal domains connected by a variable linker region [16]. IGFBPs assume a key regulatory role in many cellular processes, including proliferation, migration, differentiation, and survival. IGFBPs also play an essential role in the processes of growth, development, and tissue metabolism [17]. In the IGF axis, IGFs play influential roles in the function of IGFBPs [18,19]. Several studies indicated that IGF1 was an essential regulator of adipogenic differentiation. IGF1 was shown to upregulate phosphorylation of cAMP response element-binding protein (CREB) through the PI3K/Akt pathway, and then activated CREB increased the expression of *PPAR γ 2*, which was a crucial factor in adipogenesis through regulating specific gene expression [20–22]. IGFBP2 was the predominant binding protein secreted by differentiating white preadipocytes. In chickens, the *IGFBP2* gene could be a candidate locus or linked to a major gene associated with abdominal fat weight and percentage of abdominal fat [23,24]. Our previous research showed that, compared with dental derived stem cells, WJCMSCs exhibited decreased adipogenic differentiation potential as well as downregulated expression of *IGFBP2* [15]. These findings suggested the possible involvement of *IGFBP2* in the regulation of adipogenic differentiation in MSCs.

Many events facilitate the commitment of MSC adipogenic differentiation, including the coordination of a complex network of transcription factors, co-factors, and pathway signaling intermediates. The extracellular regulated protein kinases (ERK), p38, and JNK MAPK family are a group of serine/threonine kinases that transduce extracellular signals to intracellular targets, involving a series of protein kinase cascades and long-term response that play a crucial role in regulating cell differentiation [25–27]. Many researches focused on the effect of the MAPK family on adipogenic differentiation. Sale et al. found that ERK1 and ERK2 were required for differentiation of 3T3-L1 fibroblasts to adipocytes [28]. And inhibited ERK pathway by specific inhibitor could restrain adipocyte differentiation ability [29]. In addition, ERK activity was essential for the expressions of the *PPAR γ* and *C/EBP* [30,31]. Moreover, cells

isolated from *Erk*^{-/-} mouse showed impaired adipogenesis capability [32]. It was previously reported that the JNK pathway also regulated adipogenesis differentiation of MSCs [33]. JNK could phosphorylate PPAR γ 2 by oxidized low-density lipoprotein [34]. Yet, using SP600125, a specific JNK inhibitor, could increase the expressions of *CEBP α / β* and *PPAR γ 2*, and stimulate adipogenesis of hASCs in a dose-dependent manner [35]. Moreover, the drug for preventing osteoporosis, alendronate, inhibited adipogenic differentiation by ERK and JNK pathway in BMSCs [36]. As for the role of p38 in adipogenic differentiation, some studies showed that using p38 inhibitors could block adipocyte differentiation [37,38]. In addition, the Akt signaling pathway was also essential for inducing *PPAR γ* . Akt activity sustained the adipogenic differentiation of ASCs. *Akt* knockout mice showed impaired adipogenesis [39–41]. Importantly, *IGFBP2* could activate multiple MAPK pathways. *IGFBP2/Integrin5* interaction promoted glioma cells migration through JNK activation [42]. Exogenous *IGFBP2* induced proliferation and activated the ERK pathway in NIH-OVCAR3 cells, and also promoted proliferation in rat growth plate chondrocytes via MAPK/ERK pathway [43]. In addition, the expression of *IGFBP2* was positively regulated by PI3K/Akt pathway, and the Akt signal transduction was impaired in *Igfbp2*^{-/-} mouse cells [44]. However, it is still unknown the effect of *IGFBP2* on MAPK and Akt pathways during adipogenic differentiation of WJCMSCs. Based on the available information, we hypothesize that *IGFBP2* affects the function of MSCs, but its function and mechanism remain unclear. Here, we investigate the effects and underlying mechanisms of *IGFBP2* in the adipogenic differentiation of MSCs. Our results show overexpression *IGFBP2* enhances adipogenic differentiation of WJCMSCs by activating JNK and Akt signaling pathway. Furthermore, we find that *IGFBP2* is negatively regulated by *BCOR*, which represses the adipogenic differentiation potential of WJCMSCs.

Materials and methods

Ethics statement and cell cultures

Between January and November 2012, patients were recruited from the [Department of Oral and Maxillofacial Surgery](#) of Beijing Stomatological Hospital, Capital Medical University. And human impacted third molars were collected from six healthy male patients (16–20 years old) under approved guidelines set by the Beijing Stomatological Hospital, Capital Medical University (Ethical Committee Agreement, Beijing Stomatological Hospital Ethics Review No. 2011–02), with written informed consent. In addition, we also obtained the informed consent from parent/guardian on behalf of minors (<18 years old). The authors had access to information that could identify individual participants during or after data collection.

Teeth were first disinfected with 75% ethanol and then washed with phosphate-buffered saline. PDLSCs were isolated, cultured, and identified as previously described [15,22]. Briefly, PDLSCs were separated from periodontal ligament in the middle one-third of the root. Subsequently, MSCs were digested in a solution of 3 mg/mL collagenase type I (Worthington Biochemical Corp., Lakewood, NJ, USA) and 4 mg/mL dispase (Roche Diagnostics Corp., Indianapolis, IN, USA) for 1 h at 37°C. Single-cell suspensions were obtained by cell passage through a 70- μ m strainer (Falcon, BD Labware, Franklin Lakes, NJ, USA). Human BMSCs, ASCs, and WJCMSCs were purchased from ScienCell Research Laboratories (Carlsbad, CA, USA). MSCs were grown in a humidified, 5% CO₂ incubator at 37°C in DMEM alpha modified Eagle's medium (Invitrogen, Carlsbad, CA, USA), supplemented with 15% fetal bovine serum (FBS; Invitrogen, Carlsbad, CA, USA), 2 mmol/L glutamine, 100 U/mL penicillin and 100 μ g/mL streptomycin (Invitrogen, Carlsbad, CA, USA). The culture medium was changed every 3 days. MSCs at passages 3–5 were used in subsequent experiments. Human embryonic kidney 293T cells were maintained in complete DMEM with 10% FBS, 100 U/mL penicillin,

and 100 µg/mL streptomycin. For viral packaging, HEK293T cells at 80% confluency were co-transfected with plasmids and transfection reagent. For SP600125 (Cell Signaling Technology, Beverly, MA, USA), LY294002 (Cell Signaling Technology, Beverly, MA, USA), anisomycin (Cell Signaling Technology, Beverly, MA, USA), or insulin (Sigma-Aldrich, St. Louis, MO, USA) treatment, MSCs were starved for 24 h to synchronize the cells in DMEM alpha modified Eagle's medium without serum, then changed to routine culture medium and treated with appropriate agents. The studies on human MSCs were conducted between May 2012 and November 2016. All cell-based experiments were repeated three times. <http://dx.doi.org/10.17504/protocols.io.iegcbbw>.

Plasmid construction and viral infection

The plasmids were constructed using standard methods; all sequences were verified by appropriate restriction digestion and/or sequencing. Human full-length *IGFBP2* cDNA from ASCs fused to a M2-Flag tag was produced with a standard PCR protocol. This sequence (Flag-*IGFBP2*) was subcloned into the pQCXIN retroviral vector with AgeI and BglII restriction sites. Similarly, the human full-length *BCOR* cDNA was fused to a Flag tag (Flag-*BCOR*) and subcloned into the pQCXIN retroviral vector with AgeI and BamHI restriction sites. For viral infections, MSCs were plated overnight, and then infected with retroviruses in the presence of polybrene (6 µg/mL, Sigma-Aldrich, St. Louis, MO, USA) for 12 h. After 48 h, infected cells were selected with 600 µg/mL G418 for 10 days. <http://dx.doi.org/10.17504/protocols.io.iehcbb6>.

Western Blot analysis

Cells were lysed in RIPA buffer (10 mM Tris-HCl, 1 mM EDTA, 1% sodium dodecyl sulfate [SDS], 1% NP-40, 1:100 proteinase inhibitor cocktail, 50 mM β-glycerophosphate, 50 mM sodium fluoride). The samples were separated on a 10% SDS polyacrylamide gel and transferred to PVDF membranes with a semi-dry transfer apparatus (Bio-Rad, Hercules, CA, USA). The membranes were blotted with 5% dehydrated milk for 1 h and then incubated with primary antibodies overnight. The immune complexes were incubated with horseradish peroxidase-conjugated anti-rabbit or anti-mouse IgG (Promega, Madison, WI, USA) and visualized with SuperSignal reagents (Pierce, Rockford, IL, USA). Primary antibodies were purchased from following commercial sources: monoclonal anti-FLAG M2 (Clone No.9A3, Cat No.8146, Cell Signaling Technology, Beverly, MA, USA); monoclonal antibody against SAPK/JNK (Cat No. 9253, Cell Signaling Technology, Beverly, MA, USA); monoclonal antibody against phospho-SAPK/JNK (Cat No. 4668, Cell Signaling Technology, Beverly, MA, USA); monoclonal antibody against Akt (Cat No. 4685, Cell Signaling Technology, Beverly, MA, USA); polyclonal antibody against phospho-Akt (Cat No. 9271, Cell Signaling Technology, Beverly, MA, USA); monoclonal antibody against ERK1/2 and MAPK (Cat No. 4695, Cell Signaling Technology, Beverly, MA, USA); monoclonal antibody against phospho-p44/42 MAPK (Cat No. 4377, Cell Signaling Technology, Beverly, MA, USA); monoclonal antibody against p38 MAPK (Cat No. 8690, Cell Signaling Technology, Beverly, MA, USA); monoclonal antibody against phospho-p38 MAPK (Cat No. 4631, Cell Signaling Technology, Beverly, MA, USA). We also used a primary monoclonal antibody to detect the housekeeping protein, glyceraldehyde 3-phosphate dehydrogenase (GAPDH; Clone No. GAPDH 71.1, Cat No. G8795, Sigma-Aldrich, St. Louis, MO, USA). <http://dx.doi.org/10.17504/protocols.io.iejcbcn>.

Oil Red O staining

Adipogenic differentiation was induced by using the StemPro adipogenesis differentiation kit (Invitrogen, Carlsbad, CA, USA). MSCs were grown in the adipose-inducing medium for 3

weeks. For Oil Red O staining, after induction, cells were fixed with 10% formalin for at least 1 h at room temperature. Next, cells were stained with the 60% Oil Red O in isopropanol as working solution for 10 min. The proportion of Oil Red O-positive cells was determined by counting stained cells under a light microscope. The final OD value in each group was normalized with the total protein concentrations prepared from a duplicate plate. <http://dx.doi.org/10.17504/protocols.io.iemcbc6>.

Real-time RT-PCR

Total RNA was isolated from MSCs with TRIzol Reagent (Invitrogen, Carlsbad, CA, USA). Reverse transcription reactions contained 2 µg RNA, random hexamers or oligo (dT), and reverse transcriptase, and were performed according to the manufacturer's protocol (Invitrogen, Carlsbad, CA, USA). Real-time PCR reactions were performed using the QuantiTect SYBR Green PCR kit (Qiagen, Hilden, Germany) and an Icyler iQ Multi-color Real-time PCR Detection System with the expression of *GAPDH* as the internal control. The primers used were: *IGFBP2*, forward, 5'-cgttcaagtgcagatgtctctgaacg-3' and reverse, 5'-ggatcagcttccccgggtgttg-3'; *PPAR γ* , forward, 5'-cgagaccaacagcttctccttc tcg-3' and reverse, 5'-tttcagaaatgccttgacgtgg-3'; *LPL*, forward, 5'-cggatta acattggagaagctatccg-3' and reverse, 5'-agctggccacatctccaagtc-3'; *CD36*, forward, 5'-cgattaacataagtaaagttgccataatcg-3' and reverse, 5'-cgcagtgactt tcccaataggac-3'; *CEBPA*, forward, 5'-cggcttatacctaataactagagttgccg-3' and reverse, 5'-ggacttggtgctgcttaagatga-3'; *GAPDH*, forward, 5'-cggaccaatacga ccaaatccg-3' and reverse, 5'-agccacatcgctcagacacc-3'. The cycle threshold values (*Ct* values) were used to calculate the fold differences by the $\Delta\Delta C_t$ method. <http://dx.doi.org/10.17504/protocols.io.iencbde>.

Statistics

All statistical calculations were performed with SPSS20.0 statistical software (IBM, Armonk, NY). Comparisons between two groups were analysed by independent two-tailed Student's *t*-tests, and comparisons between more than two groups were analysed by one-way ANOVA followed by a Duncan's *post hoc* test. Data were expressed as the mean \pm standard deviation (SD) of 3 experiments per group. *P* values < 0.05 were considered statistically significant.

Results

IGFBP2 promotes adipogenic differentiation of MSCs

First, we used real-time RT-PCR to compare the *IGFBP2* mRNA levels in PDLSCs, BMSCs, ASCs, and WJCMSCs. We consistently found lower *IGFBP2* expression in WJCMSCs (0.00388 ± 0.00033) than that in PDLSCs (1 ± 0.0347), BMSCs (0.1225 ± 0.011), and ASCs (0.364 ± 0.023) (Fig 1A). Next, we investigated the *IGFBP2* expression upon adipogenic differentiation. Compared with proliferation medium, adipogenic-inducing medium induced upregulated *IGFBP2* expression in PDLSCs (Fig 1B), BMSCs (Fig 1C), ASCs (Fig 1D), and WJCMSCs (Fig 1E) at 1 and 2 weeks after induction.

To elucidate the function of *IGFBP2* in WJCMSCs, retrovirus expressing Flag-tagged wild type *IGFBP2* (Flag-*IGFBP2*) was used to perform a gain-of-function study in WJCMSCs. Ectopic *IGFBP2* overexpression was verified by real-time RT-PCR (Fig 2A) and Western Blot (Fig 2B). To examine the adipogenic differentiation potential, transduced WJCMSCs were cultured in adipose-inducing medium. Following 3 weeks induction, Oil Red O staining showed significantly more lipid deposits in WJCMSC-Flag-*IGFBP2* cells than in WJCMSC-Vector

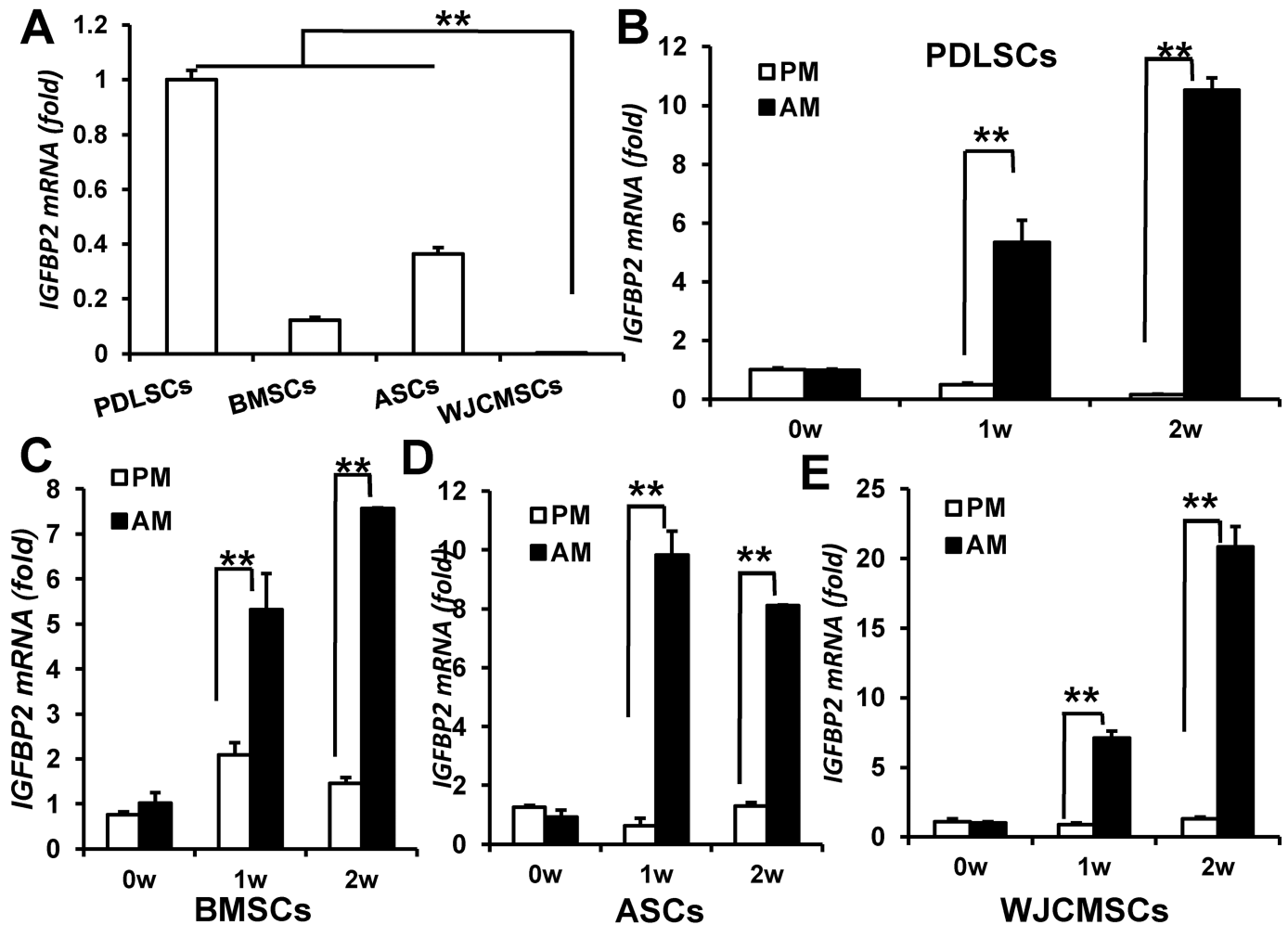


Fig 1. IGFBP2 expression levels in MSCs. (A) Real-time RT-PCR revealed that lower *IGFBP2* expression in WJCMSCs than that in PDLSCs, BMSCs, and ASCs. (B-E) Increased *IGFBP2* expression after adipogenic induction in PDLSCs (B), BMSCs (C), ASCs (D), and WJCMSCs (E). *GAPDH* was used as an internal control. ** $p < 0.01$. w: week; PM: proliferation medium; AM: adipose-inducing medium.

<https://doi.org/10.1371/journal.pone.0184182.g001>

cells (Fig 2C). After normalizing the data with total protein, these results suggested that WJCMSC-Flag-IGFBP2 cells had stronger adipogenic differentiation potential (Fig 2D). We also examined the adipogenic differentiation markers: peroxisome proliferator-activated receptor γ (*PPAR* γ), lipoprotein lipase (*LPL*), CCAAT/enhancer-binding protein α (*CEBPA*), and cluster of differentiation 36 (*CD36*). The real-time PCR results indicated *IGFBP2*-overexpressing WJCMSCs (38.9 ± 3.5) showed significantly higher *PPAR* γ mRNA levels compared with cells infected with the empty vector (23.5 ± 2.8) at 2 weeks following induction (Fig 2E). And the *LPL* (Fig 2F) and *CD36* (Fig 2G) mRNA levels were higher in WJCMSC-Flag-IGFBP2 cells at 0, 1, and 2 weeks after induction compared with WJCMSC-Vector cells. At 2 and 3 weeks after induction, Flag-IGFBP2-overexpressing WJCMSCs also showed strong induction of the *CEBPA* (Fig 2H).

To determine whether IGFBP2 had similar functions in other MSCs, we overexpressed *IGFBP2* in BMSCs via retrovirus expressing Flag-tagged wild type *IGFBP2* (S1 Fig). Assessment of Oil Red O staining and real-time RT-PCR revealed that *IGFBP2* significantly promoted adipogenic differentiation in BMSCs (S1 Fig). Together, these results showed that

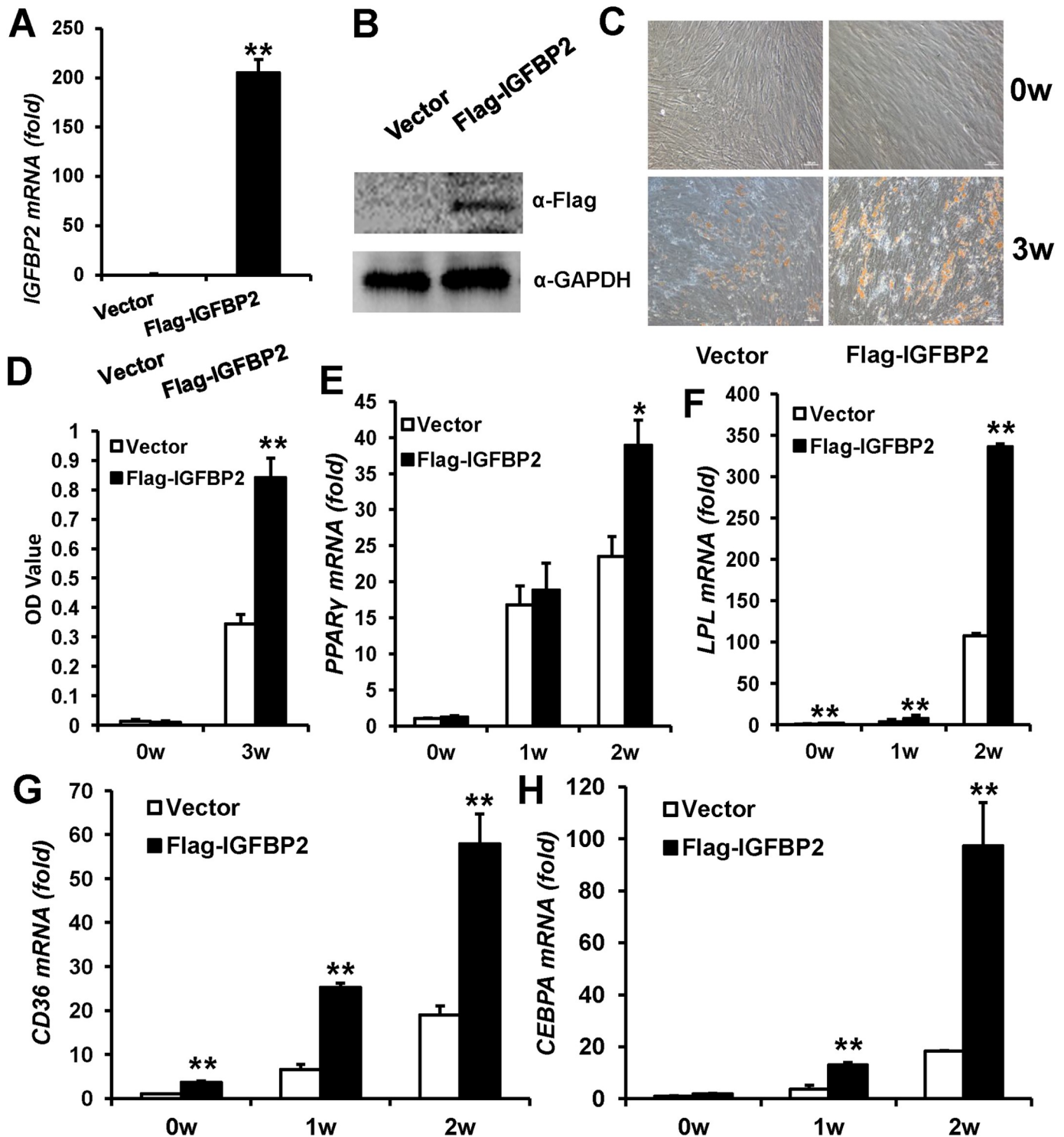


Fig 2. IGFBP2 overexpression enhances adipogenic differentiation in WJCMSCs. (A) Flag-IGFBP2-infected WJCMSCs showed *IGFBP2* overexpression by real-time RT-PCR. *GAPDH* was used as an internal control. (B) Overexpression of IGFBP2 was verified by Western Blot analysis. (C-D) Oil Red O staining and quantitative analysis showed that *IGFBP2* overexpression prompted formation of lipid deposits. Scale bar: 100 μ m. (E-H) Real-time RT-PCR showed that overexpression of *IGFBP2* upregulated expressions of *PPAR γ* (E), *LPL* (F), *CD36* (G), and *CEBPA* (H) in WJCMSCs at 0, 1, and 2 weeks after induction. *GAPDH* was used as an internal control. * $p < 0.05$. ** $p < 0.01$. α : anti; w: week.

<https://doi.org/10.1371/journal.pone.0184182.g002>

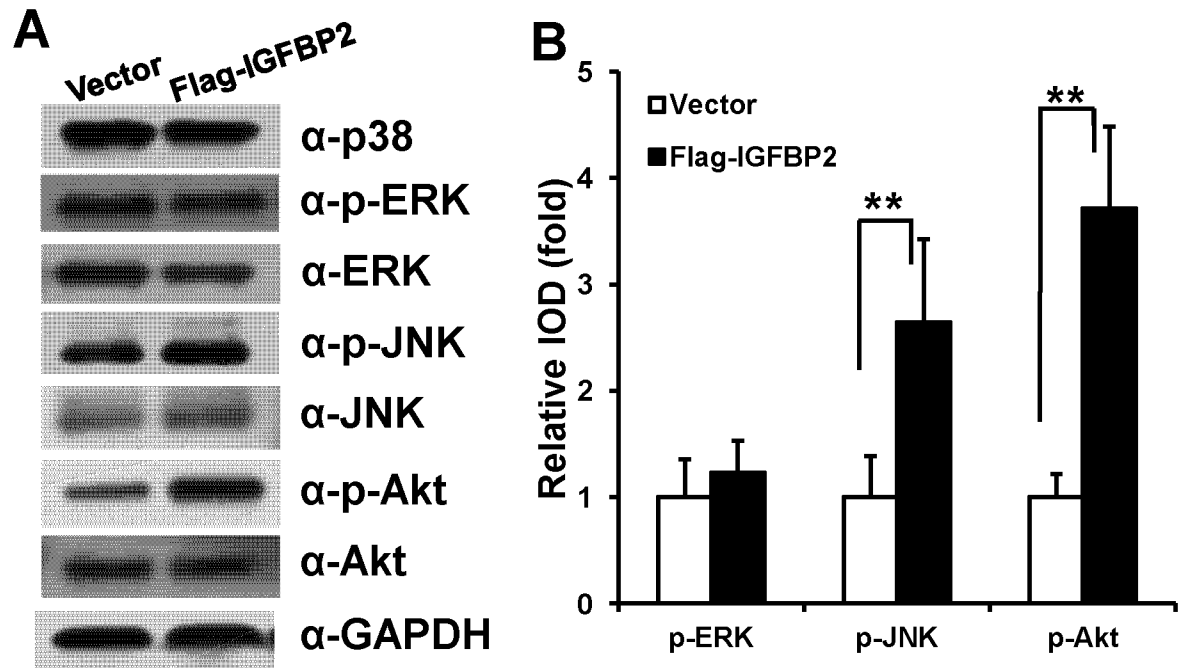


Fig 3. IGFBP2 activates JNK and Akt signaling pathways. (A) Western Blot analysis demonstrated that *IGFBP2* overexpression caused an increase in p-JNK and p-Akt in WJCMSCs, however, the total amounts of JNK, ERK, p38, and Akt proteins were not affected; The phosphorylated p38 protein was not found. (B) Quantitative analysis of p-ERK, p-JNK, and p-Akt based on Western Blot results for the WJCMSC-Flag-*IGFBP2* cells and WJCMSC-Vector cells. Total ERK, JNK, and Akt were used as internal control respectively. ** $p < 0.01$. α: anti.

<https://doi.org/10.1371/journal.pone.0184182.g003>

IGFBP2 overexpression substantially enhanced the adipogenic differentiation property of MSCs *in vitro*.

IGFBP2 increases JNK and Akt phosphorylation in WJCMSCs

To investigate how *IGFBP2* enhanced the adipogenic differentiation of WJCMSCs, we used Western Blot and quantitative analysis to examine the levels of proteins involved in MAPK signaling, including p38, ERK and JNK, and the Akt pathway. The results showed that overexpression of *IGFBP2* enhanced phosphorylation of JNK and phosphorylation of Akt in WJCMSCs, while phosphorylation of ERK, and total protein levels of p38, JNK, ERK, and Akt proteins were not affected (Fig 3A and 3B). And phosphorylated p38 MAPK was not found.

To test whether activated JNK or Akt had the capability of pro-adipogenesis in MSCs, we used the JNK activator (anisomycin) or Akt activator (insulin) in WJCMSCs. WJCMSCs were treated with 100nM, 200nM or 500nM anisomycin for 24 h to activate JNK signaling, or treated with 50nM, 100nM, 200nM or 500nM insulin for 24 h to activate Akt signaling. Western Blot results showed that 100nM, 200nM or 500nM anisomycin could effectively activate JNK signaling (S2 Fig), and 50nM, 100nM, 200nM or 500nM insulin could effectively activate Akt signaling (S2 Fig). Then, 100nM anisomycin and 50nM insulin were selected for further experiments. WJCMSCs were cultured in adipogenic-inducing medium with 100nM anisomycin or 50nM insulin. Three weeks after induction, Oil Red O staining and real-time RT-PCR results showed that 100nM anisomycin or 50nM insulin could significantly enhance the adipogenesis in WJCMSCs (S2 Fig).

IGFBP2-enhanced adipogenic differentiation of WJCMSCs is repressed by JNK or Akt inhibitors

First, WJCMSCs were treated with 10 μ M, 20 μ M, 50 μ M or 100 μ M specific JNK inhibitor, SP600125 for 48 h to block JNK signaling in WJCMSCs. Western Blot results (Fig 4A) and quantitative analysis (Fig 4B) indicated that 20 μ M, 50 μ M or 100 μ M SP600125 could effectively block JNK signaling. Then, 20 μ M SP600125 was selected for further experiments. Transduced WJCMSCs were cultured in adipogenic-inducing medium with 20 μ M SP600125. Three weeks after induction, Oil Red O staining revealed that 20 μ M SP600125 could restrain *IGFBP2*-mediated enhancement of adipogenic differentiation in WJCMSCs (Fig 4C). After normalizing the data with the total protein, the results indicated that the effect of *IGFBP2*-increased adipogenic differentiation of WJCMSCs was associated with JNK activation (Fig 4D). To confirm this finding, we further examined the adipogenic differentiation markers *PPAR γ* and *LPL* by real-time RT-PCR. The results showed that *PPAR γ* (Fig 4E) and *LPL* (Fig 4F) were significantly suppressed at 1, 2 or 3 weeks after induction in WJCMSC-Flag-*IGFBP2* + SP600125 group compared with WJCMSC-Flag-*IGFBP2* group.

Then WJCMSCs were treated with specific Akt inhibitor, LY294002, to block Akt signaling for 1 h at concentration of 10 μ M, 20 μ M, 50 μ M or 80 μ M. Western Blot results (Fig 5A) and quantitative analysis (Fig 5B) suggested that 10 μ M, 20 μ M, 50 μ M or 80 μ M LY294002 could block Akt signaling efficiently. Then, 10 μ M LY294002 was selected for further experiments. Compared with *IGFBP2*-infected cells, 10 μ M LY294002 could inhibit *IGFBP2*-mediated enhancement of adipogenic differentiation in WJCMSCs by Oil Red O staining (Fig 5C) and quantitative lipid deposit measurements (Fig 5D). And real-time RT-PCR results showed that *PPAR γ* (Fig 5E) and *LPL* (Fig 5F) were significantly suppressed at 1, 2 or 3 weeks after induction in LY294002 treated WJCMSC-Flag-*IGFBP2* group compared with untreated group.

Activated Akt signaling by IGFBP2 is repressed by the specific JNK inhibitor in WJCMSCs

To further explore the underlying mechanism, we used the specific JNK inhibitor (20 μ M SP600125) or Akt inhibitor (10 μ M LY294002) to block the activated JNK or Akt pathway by *IGFBP2* in WJCMSCs. Western Blot results (Fig 6A) and quantitative analysis (Fig 6B) showed that 20 μ M SP600125, which could inhibit the p-JNK level, effectively abrogated the expression of phosphorylation-Akt in WJCMSC-Flag-*IGFBP2* cells. However, treatment with 10 μ M LY294002 had no significant effect on the expression of p-JNK in WJCMSC-Flag-*IGFBP2* cells (Fig 6C and 6D).

BCOR negatively regulates IGFBP2 expression and inhibits adipogenic differentiation of WJCMSCs

Ectopic BCOR overexpression was confirmed by Western Blot analysis (Fig 7A). Real-time RT-PCR results showed that *BCOR* overexpression in WJCMSCs suppressed the expression of *IGFBP2* (Fig 7B). Next, to investigate adipogenic differentiation, WJCMSCs were cultured in adipogenic-inducing medium. After induction for 3 weeks, Oil Red O staining (Fig 7C) and quantitative lipid deposit measurements (Fig 7D) showed there were significantly fewer lipid deposits in WJCMSC-Flag-*BCOR* cells than in WJCMSC-Vector cells.

Discussion

Mesenchymal stem cells derived from Wharton's jelly of the umbilical cord, which are usually discarded after birth, possess multipotent abilities between those of embryonic and adult stem

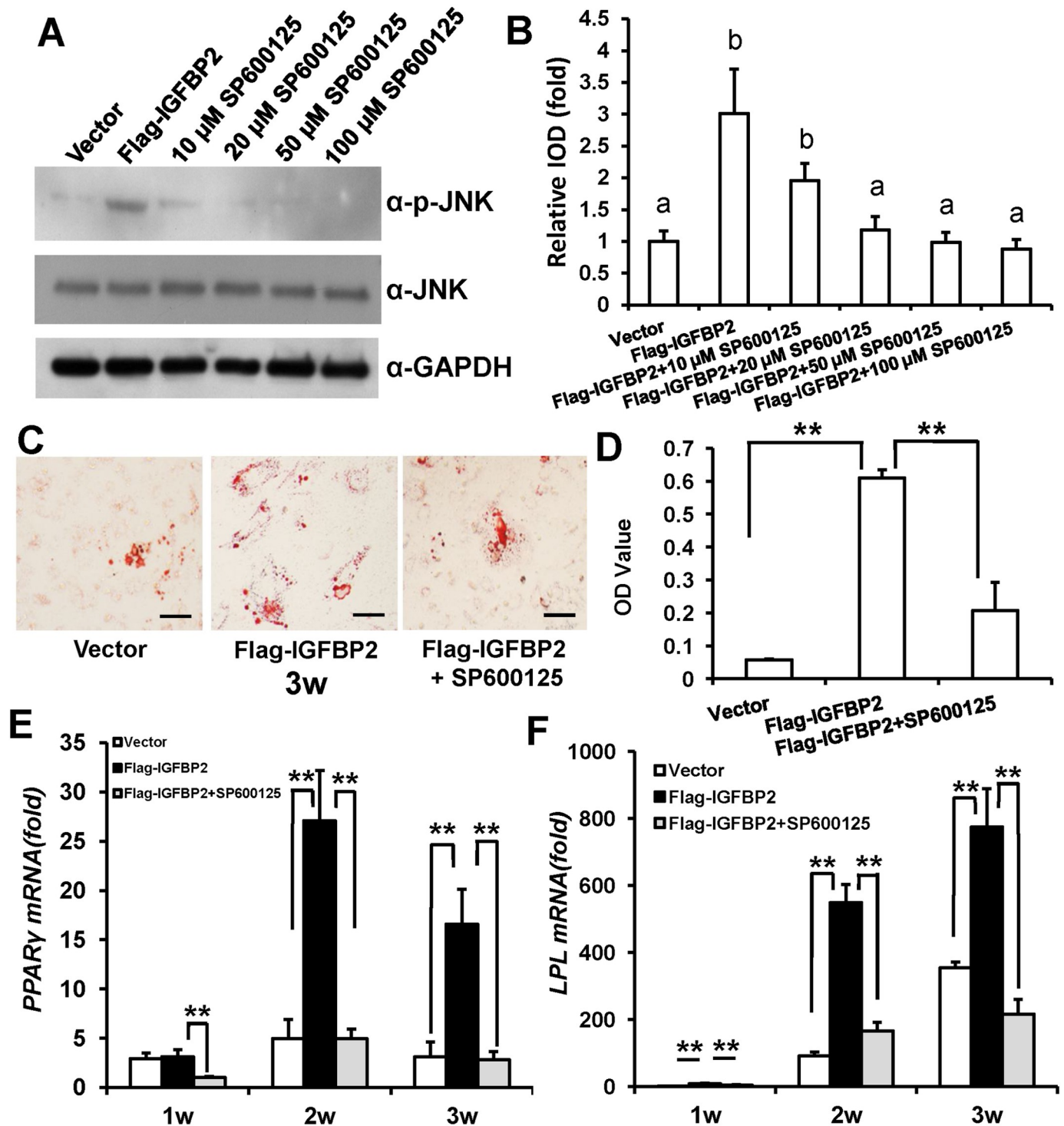


Fig 4. Effect of JNK inhibitor on IGFBP2-induced adipogenic differentiation of WJCMSCs. (A) Western Blot analysis showed a reduction of p-JNK in WJCMSC-Flag-IGFBP2 after treatment with a JNK inhibitor, SP600125 (10 μM, 20 μM, 50 μM or 100 μM in DMSO) for 48 h during adipogenic induction. (B) Quantitative analysis of p-JNK based on Western Blot results. Total JNK was used as internal control. The expression levels that are indicated with the same letter do not differ significantly. (C-D) Oil Red O staining and quantitative analysis revealed that 20 μM SP600125 effectively suppressed IGFBP2-mediated enhancement of lipid formation. Scale bar: 100 μm. (E-F) Real-time RT-PCR results showed downregulated expressions of PPARγ (E) and LPL (F) in WJCMSC-Flag-IGFBP2 cells following 20 μM SP600125 treatment during adipogenic induction at 1, 2, and 3 weeks. GAPDH was used as an internal control. ***p* < 0.01. α: anti; w: week.

<https://doi.org/10.1371/journal.pone.0184182.g004>

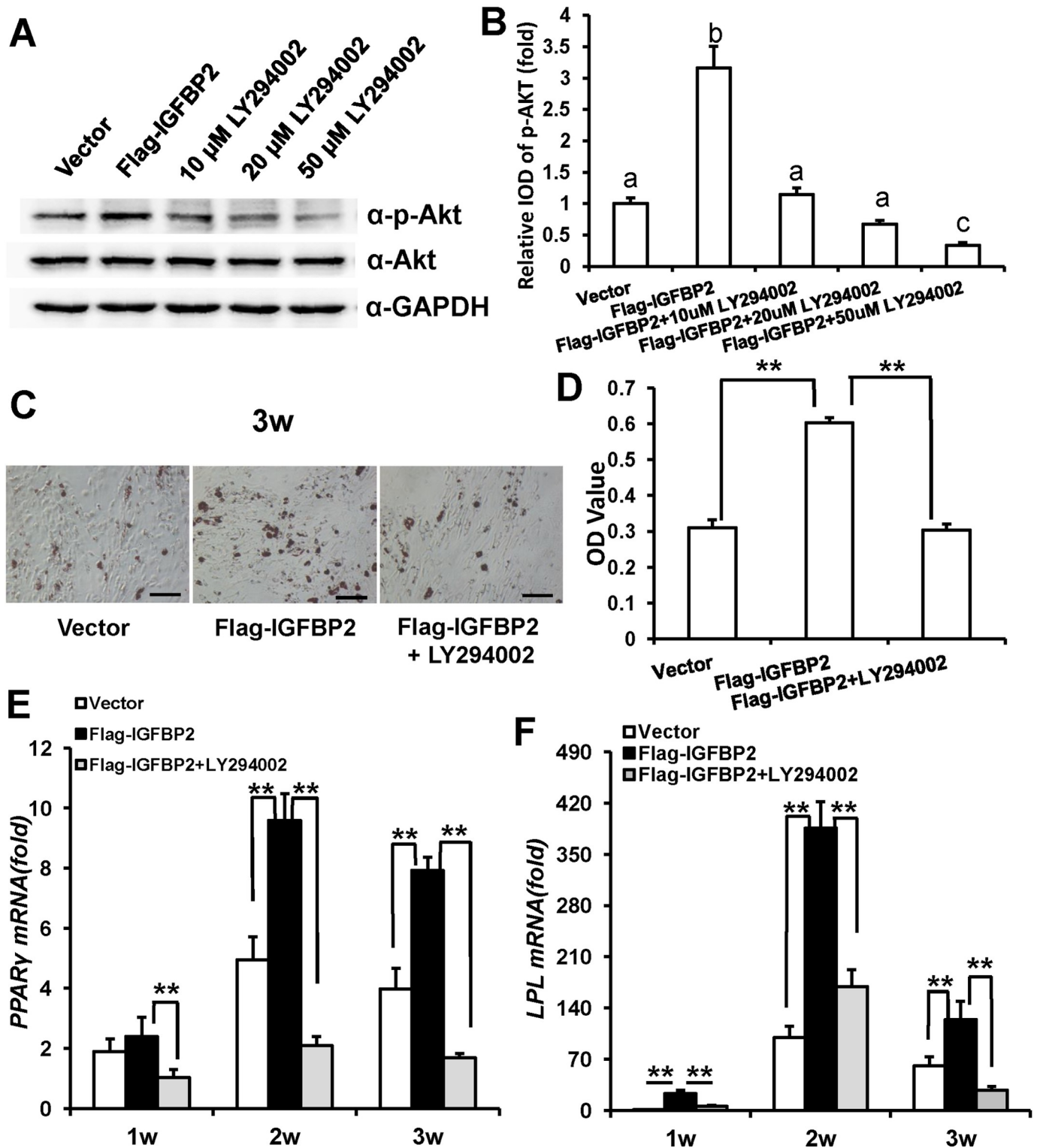


Fig 5. Effect of Akt inhibitor on IGFBP2-induced adipogenic differentiation of WJCMSCs. (A) Western Blotting results showed a reduction of p-Akt in WJCMSC-Flag-IGFBP2 following treatment with an Akt inhibitor, LY294002 (10 μM, 20 μM, 50 μM or 80 μM in DMSO) for 1 h during adipogenic induction. (B) Quantitative analysis of p-Akt based on Western Blot results. Total Akt was used as internal control. The expression levels that are indicated with the same letter do not differ significantly. (C-D) Oil Red O staining and quantitative analysis showed that 10 μM LY294002 effectively inhibited IGFBP2-mediated adipogenic differentiation. Scale bar: 100 μm. (E-F) Real-time RT-PCR results showed downregulated expressions of

PPAR γ (E) and *LPL* (F) in WJCMSC-Flag-*IGFBP2* cells following 10 μ M LY294002 treatment during adipogenic induction at 1, 2, and 3 weeks. *GAPDH* was used as an internal control. ** $p < 0.01$. α : anti; w: week.

<https://doi.org/10.1371/journal.pone.0184182.g005>

cells [2,45]. Studies have shown that WJCMSCs possess many attractive properties, including expanding faster than adult-derived MSCs, ample cell supply and the potential for autologous grafting if they are cryopreserved for future use [7,10,12]. Moreover, in clinical practice, WJCMSCs have been successfully used to treat autoimmune disease [11]. Our previous study

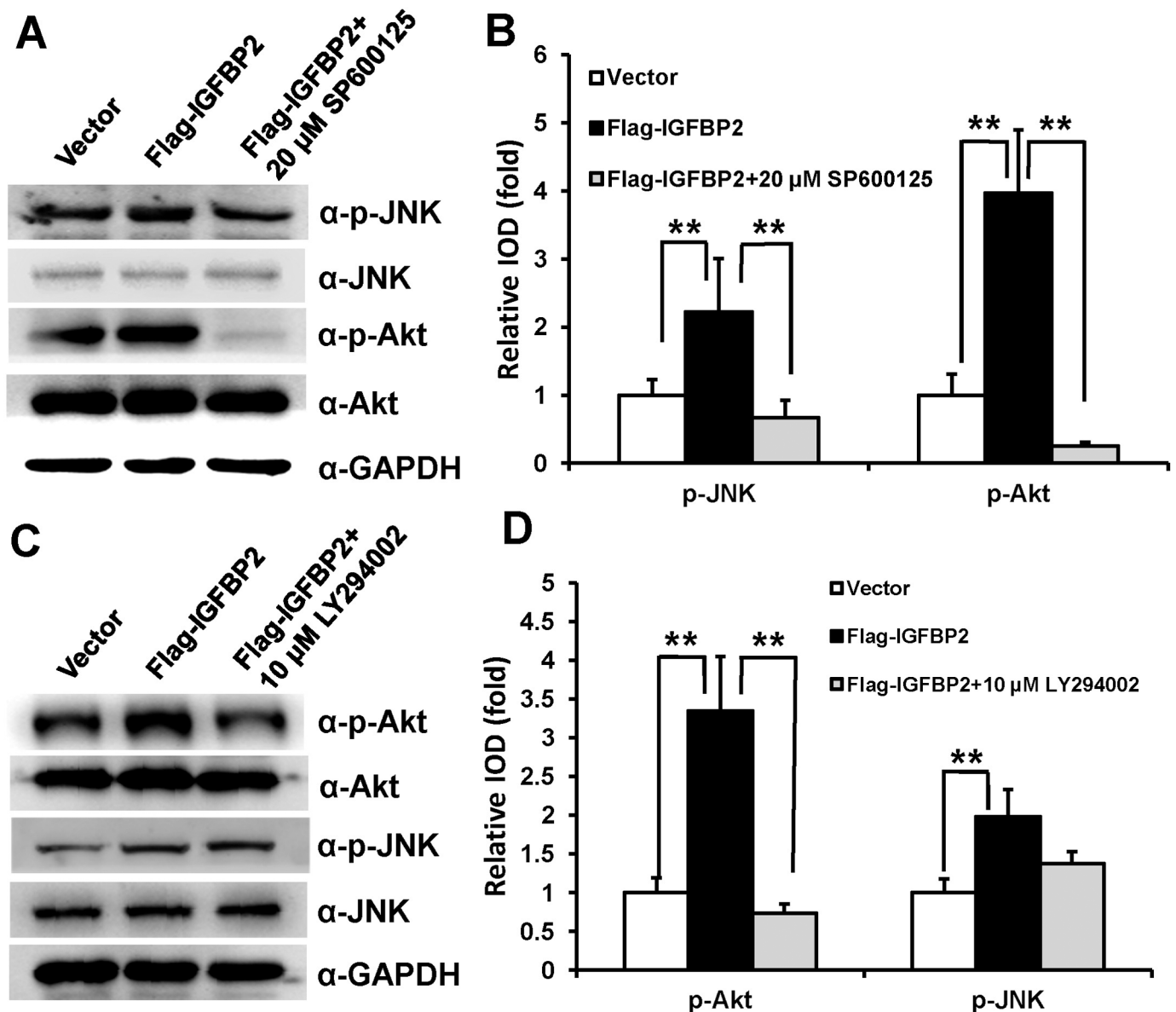


Fig 6. IGFBP2-mediated Akt activation is abrogated by JNK inhibitor. (A) Western Blot results indicated that administration of 20 μ M SP600125 decreased JNK activation and abrogated Akt phosphorylation in WJCMSC-Flag-*IGFBP2* cells. (B) Quantitative analysis of p-JNK and p-Akt based on Western Blot results for the WJCMSC-Vector cells, WJCMSC-Flag-*IGFBP2* cells, and WJCMSC-Flag-*IGFBP2* + 20 μ M SP600125 cells. Total Akt and JNK were used as internal control respectively. (C) Western Blotting results showed administration of 10 μ M LY294002 decreased the level of p-Akt activation, while had no effect on JNK phosphorylation in WJCMSC-Flag-*IGFBP2* cells. (D) Quantitative analysis of p-Akt and p-JNK based on Western Blot results. Total Akt and JNK were used as internal control respectively. ** $p < 0.01$. α : anti.

<https://doi.org/10.1371/journal.pone.0184182.g006>

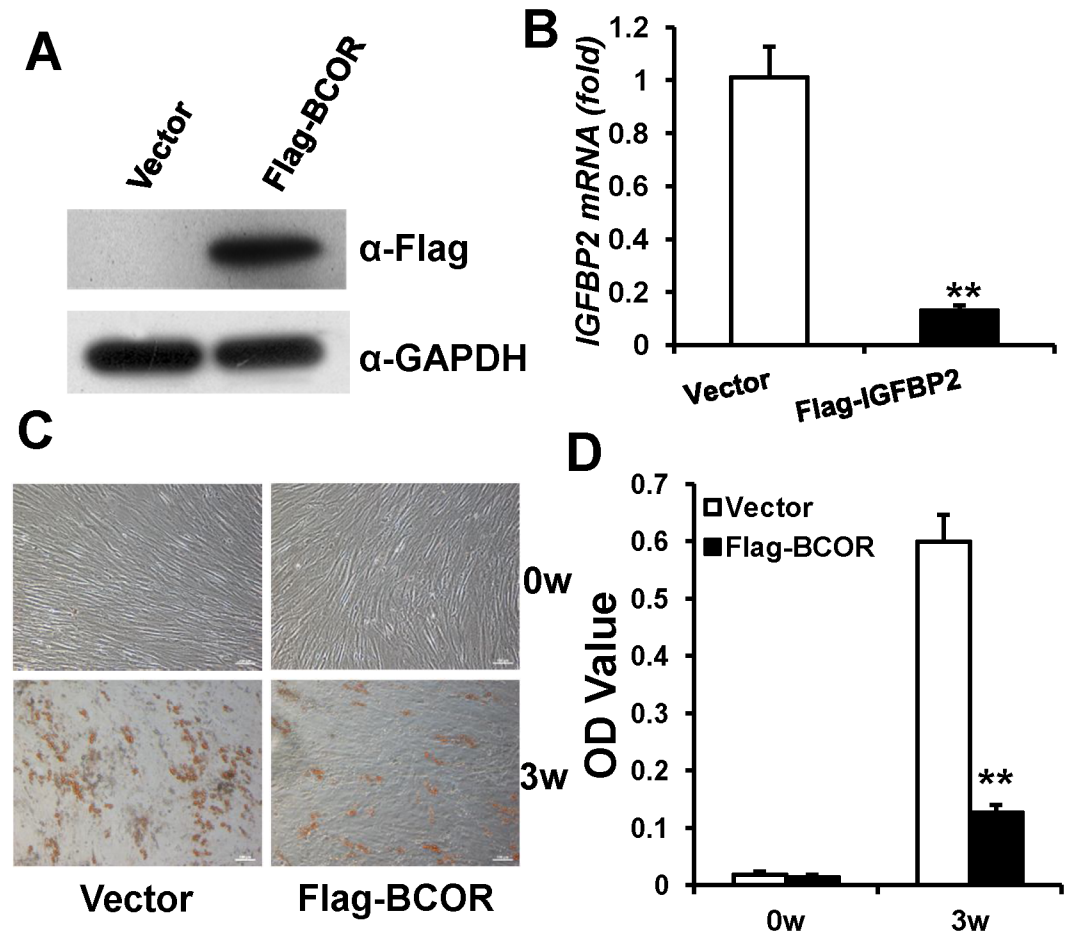


Fig 7. BCOR decreases IGFBP2 expression and weakens adipogenic differentiation in WJCMSCs. (A) Flag-BCOR-infected WJCMSCs showed BCOR overexpression, as determined by Western Blot analysis. GAPDH was used as an internal control. (B) Real-time RT-PCR analysis showed that BCOR overexpression suppressed the expression of IGFBP2 in WJCMSCs. GAPDH was used as an internal control. (C-D) Oil Red O staining and quantitative analysis showed that BCOR overexpression inhibited the formation of lipid deposits. Scale bar: 500 μ m (a, b), 100 μ m (c, d). ** $p < 0.01$. α : anti; w: week.

<https://doi.org/10.1371/journal.pone.0184182.g007>

found that compared with PDLSCs, WJCMSCs exhibited decreased adipogenic differentiation potential, and unmodified WJCMSCs might not be good seed cells for tissue regeneration [15]. Therefore, a critical issue for WJCMSCs applied in tissue engineering is how to enhance the differentiation potentials and regenerative abilities. Using microarray analysis, we observed decreased expression of IGFBP2 in WJCMSCs compared with PDLSCs [15]. IGFBP2 is mainly expressed in highly proliferative fetal tissues which represent extensive cell movement and tissue remodeling [46]. Our results confirm that IGFBP2 is a potential mediator for enhancing adipogenic differentiation of WJCMSCs and BMSCs. The potentiality of IGFBP2 and the possibility of modulating specific pathways underlying biological process of WJCMSCs offer new strategies in the field of regenerative medicine.

Regulation of adipogenic differentiation by growth factors is a complex process [20,47,48]. PPAR γ is a master regulator of adipogenesis, and generally most all pro-adipogenic signaling pathways associated with PPAR γ [49]. JNK is one of the major sub families of MAPKs [25–27]. Studies revealed that JNK pathway was associated with regulating adipogenic differentiation.

Previous research showed that wild-type *IGFBP2*-overexpressing cells showed a higher level of phosphorylation JNK [42]. In NIH-OVCAR3 cells, *IGFBP2* promoted proliferation, potentiated ERK phosphorylation and activated SAPK/JNK signaling pathway [43]. Moreover, the anti-adipogenesis effect of 6-thioinosine was mediated by decreased expression of *PPAR γ* through JNK pathway. Loss of JNK1 activity resulted in resistance to high-fat diet-induced obesity *in vivo* [50,51]. In addition, Akt was also essential for inducing *PPAR γ* and adipogenic differentiation; depletion of *Akt* impaired adipogenesis in mice [39–41]. Furthermore, impaired IGF1 mitogenesis involving the Akt pathway contributed to the distinct growth phenotype of visceral preadipocytes. More importantly, many researches inferred that using the JNK specific inhibitor or siRNA led to decreased Akt phosphorylation in many cells and cell processes [52–54]. However, it was reported that activation of JNK decreased Akt phosphorylation in liver tissue [42,43]. Pretreatment with the JNK specific inhibitor and salvianolic acid A caused decreased p-JNK and increased p-Akt in diabetic rats with ischemia/reperfusion [55]. Our results show that *IGFBP2* overexpression activates phosphorylation of JNK and Akt signaling, and activated JNK or Akt signaling enhances adipogenic differentiation of MSCs. In addition, JNK or Akt inhibitor suppresses *IGFBP2*-mediated enhancement of adipogenic differentiation in WJCMSCs. Separately, the results indicated that JNK and Akt signaling pathway exert an important role for *IGFBP2*-enhanced adipogenic differentiation. Furthermore, the specific JNK inhibitor markedly decreases the expression of phosphorylated Akt activated by *IGFBP2*, indicating that Akt is the downstream of the JNK in *IGFBP2* mediated signaling cascade. Taken together, our results confirm that *IGFBP2* enhances adipogenic differentiation of WJCMSCs via activated JNK/Akt signaling pathway. However, further study is required to investigate the regulation mechanism about JNK/Akt crosstalk in the process.

In addition to these results, we also find that *BCOR* negatively regulates the expression of *IGFBP2*; this is consistent with our previous microarray analysis, which found that *IGFBP2* was highly expressed in stem cells from the apical papilla (SCAPs) from oculo-facio-cardio-dental (OFCD) syndrome that had a mutation in *BCOR* [56]. Our results also reveal that *BCOR* represses adipogenic differentiation of WJCMSCs. The *BCOR* gene encodes a protein known as the *BCL6* co-repressor, which might use an epigenetic mechanism to direct gene silencing [56–58]. Previous researches inferred that *BCOR* regulated the function of MSCs by associating with the activating enhancer binding protein 2 alpha (*AP2 α*) promoter [56]. The 5' flanking region of *IGFBP2* gene contains motifs that might be recognized by transcription factor *AP2* [59]. Based on those studies, we speculate *BCOR* may be involved in the regulation of *IGFBP2* by epigenetics or *AP2*. However, this is beyond the scope of the current study and will require further investigation.

In summary, our results identify a novel function of *IGFBP2* in adipogenic differentiation of MSCs. Generally, *BCOR* negatively regulates *IGFBP2*, and overexpression of *IGFBP2* can enhance the adipogenic differentiation of WJCMSCs through activating JNK and Akt signaling pathways. This study elucidates molecular mechanisms underlying adipogenic differentiation of WJCMSCs, and suggests that *IGFBP2* may be a potential target to promote the adipose tissue regeneration.

Supporting information

S1 Fig. *IGFBP2* overexpression enhances adipogenic differentiation in BMSCs. (A) Flag-*IGFBP2*-infected BMSCs showed *IGFBP2* overexpression by Real-time RT-PCR. (B-C) Oil Red O staining and quantitative analysis showed that *IGFBP2* overexpression prompted formation of lipid deposits. Scale bar: 100 μ m. (D-E) Real-time RT-PCR showed that overexpression of *IGFBP2* upregulated expressions of *PPAR γ* (D) and *LPL* (E) in BMSCs after induction.

GAPDH was used as an internal control. ** $p < 0.01$. α : anti; w: week. (TIF)

S2 Fig. (A) Western Blotting results showed an accumulation of p-JNK in WJCMSCs following treatment with the JNK activator, anisomycin (100 nM, 200 nM or 500 nM in ethanol) for 24 h during adipogenic induction. (B) Quantitative analysis of p-JNK based on Western Blot results. Total JNK was used as internal control. The expression levels that are indicated with the same letter do not differ significantly. (C) Western Blotting results showed an accumulation of p-Akt in WJCMSCs following treatment with the Akt activator, insulin (50 nM, 100 nM, 200 nM or 500 nM in culture medium) for 24 h during adipogenic induction. (D) Quantitative analysis of p-Akt based on Western Blot results. Total Akt was used as internal control. The expression levels that are indicated with the same letter do not differ significantly. (E-F) Oil Red O staining and quantitative analysis showed that 100 nM anisomycin or 50 nM insulin prompted formation of lipid deposits. Scale bar: 100 μm . (G-H) Real-time RT-PCR results showed upregulated expressions of *PPAR γ* (G) and *LPL* (H) in WJCMSC cells following 100 nM anisomycin or 50 nM insulin treatment during adipogenic induction at 0 and 3 weeks. *GAPDH* was used as an internal control. ** $p < 0.01$. α : anti; w: week. (TIF)

S1 Data. This file contains all the primary data of the results in this manuscript. (ZIP)

Author Contributions

Conceptualization: Fu Wang, Yongsheng Zhou.

Data curation: Yuejun Wang.

Formal analysis: Yuejun Wang, Yunsong Liu, Zhipeng Fan, Dayong Liu, Yongsheng Zhou.

Funding acquisition: Fu Wang, Yongsheng Zhou.

Methodology: Yunsong Liu, Zhipeng Fan, Dayong Liu.

Project administration: Fu Wang, Yongsheng Zhou.

Resources: Yunsong Liu, Zhipeng Fan, Dayong Liu.

Software: Yunsong Liu, Zhipeng Fan, Dayong Liu.

Supervision: Fu Wang, Yongsheng Zhou.

Validation: Yongsheng Zhou.

Visualization: Yongsheng Zhou.

Writing – original draft: Yuejun Wang, Yongsheng Zhou.

References

1. Morikawa S, Mabuchi Y, Kubota Y, Naqai Y, Niibe K, Hiratsu E, et al. Prospective identification, isolation, and systemic transplantation of multipotent mesenchymal stem cells in murine bone marrow. *J Exp Med*. 2009; 206(11):2483–96. Epub 2009/10/19. <https://doi.org/10.1084/jem.20091046> PMID: 19841085.
2. Romanov YA, Svintsitskaya VA, Smirnov VN. Searching for alternative sources of postnatal human mesenchymal stem cells: candidate MSC-like cells from umbilical cord. *Stem Cells*. 2003; 21(1):105–10. <https://doi.org/10.1634/stemcells.21-1-105> PMID: 12529557.

3. Friedenstein AJ, Deriglasova UF, Kulagina NN, Panasuk AF, Rudakowa SF, Luriá EA, et al. Precursors for fibroblasts in different populations of hematopoietic cells as detected by the in vitro colony assay method. *Exp Hematol*. 1974; 2(2):83–92. PMID: [4455512](#).
4. Pittenger MF, Mackay AM, Beck SC, Jaiswal RK, Douglas R, Mosca JD, et al. Multilineage potential of adult human mesenchymal stem cells. *Science*. 1999; 284(5411):143–7. PMID: [10102814](#).
5. Gronthos S, Mankani M, Brahimi J, Robey PG, Shi S. Postnatal human dental pulp stem cells (DPSCs) in vitro and in vivo. *Proc Natl Acad Sci U S A*. 2000; 97(25):13625–30. <https://doi.org/10.1073/pnas.240309797> PMID: [11087820](#).
6. Seo BM, Miura M, Gronthos S, Bartold PM, Batouli S, Brahimi J, et al. Investigation of multipotent post-natal stem cells from human periodontal ligament. *Lancet*. 2004; 364(9429):149–55. [https://doi.org/10.1016/S0140-6736\(04\)16627-0](https://doi.org/10.1016/S0140-6736(04)16627-0) PMID: [15246727](#).
7. Troyer DL, Weiss ML. Wharton's jelly-derived cells are a primitive stromal cell population. *Stem Cells*. 2008; 26(3):591–9. Epub 2007/12/6. <https://doi.org/10.1634/stemcells.2007-0439> PMID: [18065397](#).
8. Wei F, Qu C, Song T, Ding G, Fan Z, Liu D, et al. Vitamin C treatment promotes mesenchymal stem cell sheet formation and tissue regeneration by elevating telomerase activity. *J Cell Physiol*. 2012; 227(9):3216–24. <https://doi.org/10.1002/jcp.24012> PMID: [22105792](#).
9. Carvalho MM, Teixeira FG, Reis RL, Sousa N, Salgado AJ. Mesenchymal stem cells in the umbilical cord: phenotypic characterization, secretome and applications in central nervous system regenerative medicine. *Curr Stem Cell Res Ther*. 2011; 6(3):221–8. PMID: [21476975](#).
10. Li DR, Cai JH. Methods of isolation, expansion, differentiating induction and preservation of human umbilical cord mesenchymal stem cells. *Chin Med J*. 2012; 125(24):4504–10. PMID: [23253727](#).
11. McGuirk JP, Smith JR, Divine CL, Zuniga M, Weiss ML. Wharton's Jelly-Derived Mesenchymal Stromal Cells as a Promising Cellular Therapeutic Strategy for the Management of Graft-versus-Host Disease. *Pharmaceuticals*. 2015; 8(2):196–220. <https://doi.org/10.3390/ph8020196> PMID: [25894816](#).
12. Wang L, Ott L, Seshareddy K, Weiss ML, Detamore MS. Musculoskeletal tissue engineering with human umbilical cord mesenchymal stromal cells. *Regen Med*. 2011; 6(1):95–109. <https://doi.org/10.2217/rme.10.98> PMID: [21175290](#).
13. Liu Y, Zheng Y, Ding G, Fang D, Zhang C, Bartold PM, et al. Periodontal ligament stem cell-mediated treatment for periodontitis in miniature swine. *Stem Cells*. 2008; 26(4):1065–73. Epub 2008/1/31. <https://doi.org/10.1634/stemcells.2007-0734> PMID: [18238856](#).
14. Liu D, Wang Y, Jia Z, Wang L, Wang J, Yang D, et al. Demethylation of IGFBP5 by Histone Demethylase KDM6B Promotes Mesenchymal Stem Cell-Mediated Periodontal Tissue Regeneration by Enhancing Osteogenic Differentiation and Anti-Inflammation Potentials. *Stem Cells*. 2015; 33(8):2523–36. Epub 2015/5/12. <https://doi.org/10.1002/stem.2018> PMID: [25827480](#).
15. Yu S, Long J, Yu J, Du J, Ma P, Ma Y, et al. Analysis of differentiation potentials and gene expression profiles of mesenchymal stem cells derived from periodontal ligament and Wharton's jelly of the umbilical cord. *Cells Tissues Organs*. 2013; 197(3):209–23. Epub 2012/12/14. <https://doi.org/10.1159/000343740> PMID: [23257615](#).
16. Forbes BE, McCarthy P, Norton RS. Insulin-like growth factor binding proteins: a structural perspective. *Front Endocrinol*. 2012; 3:38. <https://doi.org/10.3389/fendo.2012.00038> PMID: [22654863](#).
17. Baxter RC, Martin JL. Binding proteins for the insulin-like growth factors: structure, regulation and function. *Prog Growth Factor Res*. 1989; 1(1):49–68. PMID: [2485012](#).
18. Clemmons DR. Use of mutagenesis to probe IGF-binding protein structure/function relationships. *Endocr Rev*. 2001; 22(6):800–17. <https://doi.org/10.1210/edrv.22.6.0449> PMID: [11739334](#).
19. Laviola L, Natalicchio A, Giorgino F. The IGF-I signaling pathway. *Curr Pharm Des*. 2007; 13(7):663–9. PMID: [17346182](#).
20. Rosen ED, MacDougald OA. Adipocyte differentiation from the inside out. *Nat Rev Mol Cell Biol*. 2006; 7(12):885–96. <https://doi.org/10.1038/nrm2066> PMID: [17139329](#).
21. Smith PJ, Wise LS, Berkowitz R, Wan C, Rubin CS. Insulin-like growth factor-I is an essential regulator of the differentiation of 3T3-L1 adipocytes. *J Biol Chem*. 1988; 263(19):9402–8. PMID: [2967822](#).
22. Liu J, Chen L, Zhou Y, Liu X, Tang K. Insulin-like growth factor-1 and bone morphogenetic protein-2 jointly mediate prostaglandin E2-induced adipogenic differentiation of rat tendon stem cells. *PLoS One*. 2014; 9(1):e85469. <https://doi.org/10.1371/journal.pone.0085469> PMID: [24416413](#).
23. Boney CM, Moats-Staats BM, Stiles AD, D'Ercole AJ. Expression of insulin-like growth factor-I (IGF-I) and IGF-binding proteins during adipogenesis. *Endocrinology*. 1994; 135(5):1863–8. <https://doi.org/10.1210/endo.135.5.7525256> PMID: [7525256](#).
24. Leng L, Wang S, Li Z, Wang Q, Li H. A polymorphism in the 3'-flanking region of insulin-like growth factor binding protein 2 gene associated with abdominal fat in chickens. *Poult Sci*. 2009; 88(5):938–42. <https://doi.org/10.3382/ps.2008-00453> PMID: [19359680](#).

25. James AW. Review of signaling pathways governing MSC osteogenic and adipogenic differentiation. *Scientifica*. 2013; 2013:684736. Epub 2013/12/12. <https://doi.org/10.1155/2013/684736> PMID: [24416618](https://pubmed.ncbi.nlm.nih.gov/24416618/).
26. Yang SH, Sharrocks AD, Whitmarsh AJ. MAP kinase signalling cascades and transcriptional regulation. *Gene*. 2013; 513(1):1–13. Epub 2012/11/1. <https://doi.org/10.1016/j.gene.2012.10.033> PMID: [23123731](https://pubmed.ncbi.nlm.nih.gov/23123731/).
27. Katz M, Amit I, Yarden Y. Regulation of MAPKs by growth factors and receptor tyrosine kinases. *Biochim Biophys Acta*. 2007; 1773(8):1161–76. Epub 2007/1/10. <https://doi.org/10.1016/j.bbamcr.2007.01.002> PMID: [17306385](https://pubmed.ncbi.nlm.nih.gov/17306385/).
28. Sale EM, Atkinson PG, Sale GJ. Requirement of MAP kinase for differentiation of fibroblasts to adipocytes, for insulin activation of p90 S6 kinase and for insulin or serum stimulation of DNA synthesis. *EMBO J*. 1995; 14(4):674–84. PMID: [7882971](https://pubmed.ncbi.nlm.nih.gov/7882971/).
29. Tang QQ, Otto TC, Lane MD. Mitotic clonal expansion: a synchronous process required for adipogenesis. *Proc Natl Sci U S A*. 2003; 100(1):44–49. Epub 2002/12/26. <https://doi.org/10.1073/pnas.0137044100> PMID: [12502791](https://pubmed.ncbi.nlm.nih.gov/12502791/).
30. Aubert J, Dessolin S, Belmonte N, Li M, McKenzie FR, Staccini L, et al. Leukemia inhibitory factor and its receptor promote adipocyte differentiation via the mitogen-activated protein kinase cascade. *J Biol Chem*. 1999; 274(35):24965–72. PMID: [10455174](https://pubmed.ncbi.nlm.nih.gov/10455174/).
31. Bost F, Caron L, Marchetti I, Dani C, Le Marchand-Brustel Y, Binétry B. Retinoic acid activation of the ERK pathway is required for embryonic stem cell commitment into the adipocyte lineage. *Biochem J*. 2002; 361(Pt3):621–7. PMID: [11802792](https://pubmed.ncbi.nlm.nih.gov/11802792/).
32. Bost F, Aouadi M, Caron L, Even P, Belmonte N, Prot M, et al. The extracellular signal-regulated kinase isoform ERK1 is specifically required for in vitro and in vivo adipogenesis. *Diabetes*. 2005; 54(2):402–11. PMID: [15677498](https://pubmed.ncbi.nlm.nih.gov/15677498/).
33. Tominaga S, Yamaguchi T, Takahashi S, Hirose F, Osumi T. Negative regulation of adipogenesis from human mesenchymal stem cells by Jun N-terminal kinase. *Biochem Biophys Res Commun*. 2005; 326(2):499–504. <https://doi.org/10.1016/j.bbrc.2004.11.056> PMID: [15582605](https://pubmed.ncbi.nlm.nih.gov/15582605/).
34. Yin R, Dong YG, Li HL. PPARgamma phosphorylation mediated by JNK MAPK: a potential role in macrophage-derived foam cell formation. *Acta Pharmacol Sin*. 2006; 27(9):1146–52. <https://doi.org/10.1111/j.1745-7254.2006.00359.x> PMID: [16923334](https://pubmed.ncbi.nlm.nih.gov/16923334/).
35. Gu H, Huang Z, Yin X, Zhang J, Gong L, Chen J, et al. Role of c-Jun N-terminal kinase in the osteogenic and adipogenic differentiation of human adipose-derived mesenchymal stem cells. *Exp Cell Res*. 2015; 339(1):112–21. Epub 2015/8/10. <https://doi.org/10.1016/j.yexcr.2015.08.005> PMID: [26272544](https://pubmed.ncbi.nlm.nih.gov/26272544/).
36. Fu L, Tang T, Miao Y, Zhang S, Qu Z, Dai K. Stimulation of osteogenic differentiation and inhibition of adipogenic differentiation in bone marrow stromal cells by alendronate via ERK and JNK activation. *Bone*. 2008; 43(1):40–7. Epub 2008/3/29. <https://doi.org/10.1016/j.bone.2008.03.008> PMID: [18486585](https://pubmed.ncbi.nlm.nih.gov/18486585/).
37. Engelman JA, Lisanti MP, Scherer PE. Specific inhibitors of p38 mitogen-activated protein kinase block 3T3-L1 adipogenesis. *J Biol Chem*. 1998; 273(48):32111–20. PMID: [9822687](https://pubmed.ncbi.nlm.nih.gov/9822687/).
38. Patel NG, Holder JC, Smith SA, Kumar S, Eggo MC. Differential regulation of lipogenesis and leptin production by independent signaling pathways and rosiglitazone during human adipocyte differentiation. *Diabetes*. 2003; 52(1):43–50. PMID: [12502492](https://pubmed.ncbi.nlm.nih.gov/12502492/).
39. Cervelli V, Scioli MG, Gentile P, Doldo E, Bonanno E, Spagnoli LG, et al. Platelet-rich plasma greatly potentiates insulin-induced adipogenic differentiation of human adipose-derived stem cells through a serine/threonine kinase Akt-dependent mechanism and promotes clinical fat graft maintenance. *Stem Cells Transl Med*. 2012; 1(3):206–20. Epub 2012/3/7. <https://doi.org/10.5966/sctm.2011-0052> PMID: [23197780](https://pubmed.ncbi.nlm.nih.gov/23197780/).
40. Peng XD, Xu PZ, Chen ML, Hahn-Windgassen A, Skeen J, Jacobs J, et al. Dwarfism, impaired skin development, skeletal muscle atrophy, delayed bone development, and impeded adipogenesis in mice lacking Akt1 and Akt2. *Genes Dev*. 2003; 17(11):1352–65. <https://doi.org/10.1101/gad.1089403> PMID: [12782654](https://pubmed.ncbi.nlm.nih.gov/12782654/).
41. Xu J, Liao K. Protein kinase B/Akt 1 plays a pivotal role in insulin-like growth factor-1 receptor signaling induced 3T3-L1 adipocyte differentiation. *J Biol Chem*. 2004; 279(34):35914–22. Epub 2004/6/10. <https://doi.org/10.1074/jbc.M402297200> PMID: [15192111](https://pubmed.ncbi.nlm.nih.gov/15192111/).
42. Mendes KN, Wang GK, Fuller GN, Zhang W. JNK mediates insulin like growth factor binding protein 2/ integrin alpha5-dependent glioma cell migration. *Int J Onco*. 2010; 37(1):143–53. PMID: [20514406](https://pubmed.ncbi.nlm.nih.gov/20514406/).
43. Chakrabarty S, Kondratick L. Insulin-like growth factor binding protein-2 stimulates proliferation and activates multiple cascades of the mitogen-activated protein kinase pathways in NIH-OVCAR3 human epithelial ovarian cancer cells. *Cancer Biol Ther*. 2006; 5(2):189–97. Epub 2006/2/15. PMID: [16357519](https://pubmed.ncbi.nlm.nih.gov/16357519/).

44. Mehrian-Shai R, Chen CD, Shi T, Horvath S, Nelson SF, Reichardt JK, et al. Insulin growth factor-binding protein 2 is a candidate biomarker for PTEN status and PI3K/Akt pathway activation in glioblastoma and prostate cancer. *Proc Natl Acad Sci U S A*. 2007; 104(13):5563–8. Epub 2007/3/19. <https://doi.org/10.1073/pnas.0609139104> PMID: 17372210.
45. Nekanti U, Dastidar S, Venugopal P, Totey S, Ta M. Increased proliferation and analysis of differential gene expression in human Wharton's jelly-derived mesenchymal stromal cells under hypoxia. *Int J Biol Sci*. 2010; 6(5):499–512. PMID: 20877435.
46. Green BN, Jones SB, Streck RD, Wood TL, Rotwein P, Pintar JE. Distinct expression patterns of insulin-like growth factor binding proteins 2 and 5 during fetal and postnatal development. *Endocrinology*. 1994; 134(2):954–62. <https://doi.org/10.1210/endo.134.2.7507840> PMID: 7507840.
47. Luchetti F, Canonico B, Bartolini D, Arcangeletti M, Cifollilli S, Murdolo G, et al. Melatonin regulates mesenchymal stem cell differentiation: a review. *J Pineal Res*. 2014; 56(4):382–97. Epub 2014/4/15. <https://doi.org/10.1111/jpi.12133> PMID: 24650016.
48. Zamani N, Brown CW. Emerging roles for the transforming growth factor-beta superfamily in regulating adiposity and energy expenditure. *Endocr Rev*. 2011; 32(3):387–403. Epub 2010/12/20. <https://doi.org/10.1210/er.2010-0018> PMID: 21173384.
49. Rosen ED, Walkey CJ, Puiqsriver P, Spiegelman BM. Transcriptional regulation of adipogenesis. *Genes Dev*. 2000; 14(11):1293–307. PMID: 10837022.
50. Hirosumi J, Tuncman G, Chang L, Görgün CZ, Uysal KT, Maeda K, et al. A central role for JNK in obesity and insulin resistance. *Nature*. 2002; 420(6913):333–6. <https://doi.org/10.1038/nature01137> PMID: 12447443.
51. Lee J, Jung E, Lee J, Huh S, Kim YS, Kim YW, et al. Anti-adipogenesis by 6-thioinosine is mediated by downregulation of PPAR gamma through JNK-dependent upregulation of Inos. *Cell Mol Life Sci*. 2010; 67(3):467–81. Epub 2009/11/26. <https://doi.org/10.1007/s00018-009-0196-y> PMID: 19941061.
52. Shaw J, Kirshenbaum LA. Prime time for JNK-mediated Akt reactivation in hypoxia-reoxygenation. *Circ Res*. 2006; 98(1):7–9. <https://doi.org/10.1161/01.RES.0000200397.22663.b6> PMID: 16397151.
53. Taniguchi CM, Aleman JO, Ueki K, Luo J, Asano T, Kaneto H, et al. The p85alpha regulatory subunit of phosphoinositide 3-kinase potentiates c-Jun N-terminal kinase-mediated insulin resistance. *Mol Cell Biol*. 2007; 27(8):2830–40. Epub 2007/2/5. <https://doi.org/10.1128/MCB.00079-07> PMID: 17283057.
54. Shao Z, Bhattacharya K, Hsieh E, Park L, Walters B, Germann U, et al. c-Jun N-terminal kinases mediate reactivation of Akt and cardiomyocyte survival after hypoxic injury in vitro and in vivo. *Circ Res*. 2006; 98(1):111–8. Epub 2005/11/23. <https://doi.org/10.1161/01.RES.0000197781.20524.b9> PMID: 16306447.
55. Chen Q, Xu T, Li D, Pan D, Wu P, Luo T, et al. JNK/PI3K/Akt signaling pathway is involved in myocardial ischemia/reperfusion injury in diabetic rats: effects of salvianolic acid A intervention. *Am J Transl Res*. 2016; 8(6):2534–48. PMID: 27398138.
56. Fan Z, Yamaza T, Lee JS, Yu J, Wang S, Fan G, et al. BCOR regulates mesenchymal stem cell function by epigenetic mechanisms. *Nat Cell Biol*. 2009; 11(8):1002–9. Epub 2009/7/5. <https://doi.org/10.1038/ncb1913> PMID: 19578371.
57. Huynh KD, Fischle W, Verdin E, Bardwell VJ. BCoR, a novel corepressor involved in BCL-6 repression. *Genes Dev*. 2000; 14(14):1810–23. PMID: 10898795.
58. Dong R, Yao R, Du J, Wang S, Fan Z. Depletion of histone demethylase KDM2A enhanced the adipogenic and chondrogenic differentiation potentials of stem cells from apical papilla. *Exp Cell Res*. 2013; 319(18):2874–82. Epub 2013/7/18. <https://doi.org/10.1016/j.yexcr.2013.07.008> PMID: 23872478.
59. Brown AL, Rechler MM. Cloning of the rat insulin-like growth factor-binding protein-2 gene and identification of a functional promoter lacking a TATA box. *Mol Endocrinol*. 1990; 4(12):2039–51. <https://doi.org/10.1210/mend-4-12-2039> PMID: 1707131.